Sandwich beams with gradient-density aluminum foam cores subjected to impact loading

J. Zhang & G. P. Zhao
State Key Laboratory of Mechanical Structure Strength and Vibration, Xi'an Jiaotong University, China

Abstract

The dynamic response of end-clamped sandwich beams is predicted by loading the beams at mid-span using metal foam projectiles. The sandwich beams comprise aluminum alloy face sheets and aluminum foam cores. The aluminum foam cores, having identical areal density, exist in homogeneous core, low-high gradient-density core or high-low gradient-density core. Two-dimensional (2D) finite element (FE) models were created from tomographic images of the foam cores, which represent the cell shape and geometric distribution of the real foams. A quasi-static compressive test was carried out on a MTS machine for homogeneous aluminum foam core to obtain the mechanical properties of the gradient-density foam cell wall. A uniformly distributed pressure versus time history is employed to simulate a shock impulse involving high-speed impact of aluminium foam projectiles. Two deflected shapes of the sandwich beams are found to be bend dominated mode and stretch dominated mode according to the different initial impulse. The sandwich beams with different densities foam cores outperform monolithic solids of equivalent weight in the bend dominated domain. The benefits diminish at large deflections, as the response becomes stretch-dominated. In bend dominated domain, the sandwich beam with homogeneous foam cores shows smallest mid-point deflection of back face sheet, while smallest average compressive strain of aluminum foams cores occurs in sandwich beams with high-low gradient-density foam cores.
Keywords: cellular solid, impact loading, blast resistance, dynamic simulations.

WIT Transactions on The Built Environment, Vol 141, © 2014 WIT Press
www.witpress.com, ISSN 1743-3509 (on-line)
doi:10.2495/SUSI140341

1 Introduction

High porosity metal foam-cored sandwich structures, including sandwich beams, plates and shells, provide superior static and dynamic performance relative to monolithic structures of equal mass. These lightweight sandwich structures are commonly used in transportation systems, such as aircrafts, high-speed trains and ships, for energy absorption and blast protection purposes. Significant research efforts have been directed towards understanding the dynamic responses of these novel sandwich structures. Radford *et al*. [1] developed an experimental technique to simulate water and air shock loading on sandwich structures using metal foam projectiles, and demonstrated that metal foam-cored sandwich beams or plates had a higher shock resistance than that of the monolithic beam or plate of equal mass [2, 3]. This shock loading technique is subsequently employed by many researchers to explore the dynamic resistance of sandwich structures having homogeneous metal foam cores.

The potential of sandwich structures with gradient-density foam cores was recently demonstrated by Daxner *et al*. [4], but only limited experimental data exist such structures. Brothers and Dunand [5] measured the compressive mechanical properties of both homogeneous and gradient-density Al-6061 foams. While the homogeneous foam showed a near constant plateau stress, the gradient-density foam exhibited a smoothly rising plateau stress. Wang *et al*. [6] performed shock tube experiments to study the dynamic response of sandwich panels with E-Glass Vinyl Ester (EVE) composite facesheets and stepwise gradient styrene foam cores whilst Zhao *et al*. [7] studied the perforation behavior of sandwich plates with gradient-density polymeric hollow sphere cores under impact loading.

Much less is known about the dynamic responses of sandwich structures with gradient-density metal foam cores to shock load. Although finite element (FE) simulations have been performed to investigate the shock response of sandwich structures with gradient-density foam cores [8] the calculations were restricted to simple gradient-density foams: the foam was divided into several homogeneous layers along the core height, with foam properties assigned individually to each layer. In this research, to avoid the side effects of discontinuous foam properties in previous studies, a continuous gradient-density aluminum foam core is created by mesoscopic FE model which represents the cell shape and geometric distribution of real foams. The main aim is to compare the dynamic performance of sandwich beams with gradient-density foam cores with that having homogeneous cores. The dynamic responses of end-clamped sandwich beams subjected to transverse shock loading at mid-span are simulated. Three types of aluminum foam core configurations having identical areal density, namely, homogeneous core, low-high gradient-density core and high-low gradient-density core, are modeled.

2 Finite element simulations

2.1 Two-dimensional model of end-clamped sandwich beam

Sandwich beams with Al-2024 aluminum alloy facesheets and closed-cell aluminum foam cores are selected to explore their transient transverse responses. The beam, clamed at both ends and shock loaded at mid-span, has a span of $2L$ = 250 mm and is comprised of two identical facesheets of thickness h = 0.5 mm and a gradient-density foam core of thickness c = 10 mm.

Two-dimensional (2D) random solid FE models of the foam core are created from tomographic images of closed-cell aluminium foams fabricated using the powder metallurgy foaming technique, inspired by 2D random Voronoi honeycomb models [9] as well as X-ray tomography models [10]. Details regarding the mesoscopic FE model can be found in a separate work [11]. The FE models for gradient-density foam core are shown in Figs. 1, along with the profiles of their relative densities along the beam height. Whilst Fig. 1 presents a linearly decreasing gradient foam configuration from the upper facesheet (the high-low gradient-density foam core), another gradient foam configuration (the low-high gradient-density core) is created by simply turning the former upside down. The average relative density of the three foam cores (homogeneous core, low-high gradient-density core, and high-low gradient-density core) is adjusted to the same value 0.3.

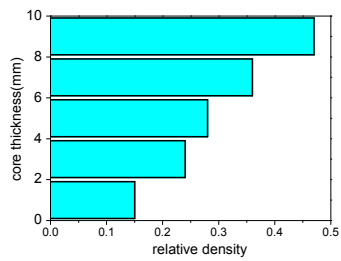

(a)

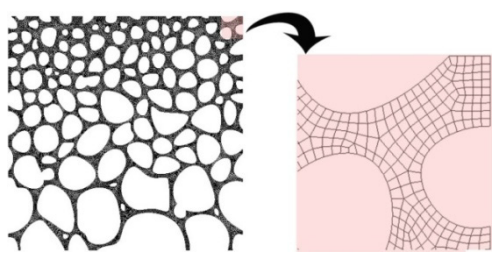

(b)

Figure 1: FE model for gradient-density foam core (a) Profile of foam relative density; (b) FE model.

Due to symmetry, only half of the sandwich beam is modeled, with the clamped boundary conditions enforced by constraining the horizontal and vertical motion of all nodes at the ends of the beam (Fig. 2). The beam is modeled by solid elements with eight nodes (solid 164). Five elements are generated for each facesheet along the thickness (see insert of Fig. 2). To model the foam core, the average element size of the cell walls is reduced to 0.40 mm so that numerical convergence is ensured. Mesh sensitivity studies reveal that additional mesh refinements do not improve the accuracy of the calculations appreciably. Whilst automatic single surface contact options are applied to enforce (potentially) hard contact between cell wall surfaces, perfect bonding (node connectivity) between the foam core and the facesheets is assumed. No imperfections in terms of material properties and other manufacturing defects are introduced. For comparison, a monolithic Al-2024 aluminum alloy beam of length 250 mm and thickness 4 mm is also modeled, which has the same mass as the foam-cored sandwich beams. The explicit FE code LS-DYDA is employed to carry out all the simulations.

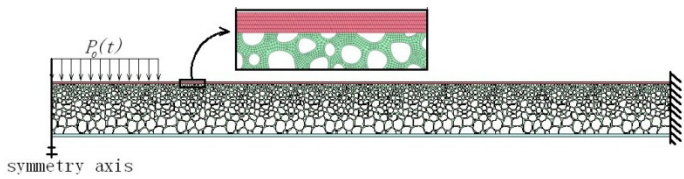

Figure 2: Two-dimensional FE model of end-clamped sandwich beam subjected to impact loading at mid-span.

2.2 Impulsive versus finite pressure loading (idealized blast loading)

It has been established [1] that metal foam projectiles exerted approximately a rectangular pressure versus time pulse of magnitude p_0 and duration τ, as follows:

$$p = \begin{cases} p_0, & 0 \le t \le \tau \\ 0, & t \ge \tau \end{cases}$$

Momentum conservation implies that the impulse is:

$$I = \int_0^\infty p(t)\,dt = p_0\tau$$

In the present study, idealized blast loading (of span $2a$ = 26.16 mm, Fig. 2) achieved using metal foam projectile is applied to all the sandwich and monolithic beams.

2.3 Constitutive description of facesheet material

The Al-2024 aluminium facesheets are represented by material model 104 of LS_DYNA [24]. This model is based on the continuum damage theory with

associated flow and von Mises yield criterion, with the effective stress $\tilde{\sigma}$ defined as:

$$\tilde{\sigma} = \frac{\sigma}{1-D}$$

where D ($0 \le D \le 1$) is the isotropic damage variable and σ is the usual true stress measure. Hardening of the material is expressed by:

$$\tilde{\sigma} = \frac{\sigma}{1-D} = Y^0 + Q_1\left(1-\exp\left(-c_1 r\right)\right) + Q_2\left(1-\exp\left(-c_2 r\right)\right)$$

where r is the damage accumulated plastic strain. Since the incremental plastic work in terms of the usual and effective stress measures has to be equal, i.e. $\tilde{\sigma}\dot{r} = \sigma\dot{\varepsilon}_{pl}$, the rate of the damage accumulated strain is given by:

$$\dot{r} = \left(1-D\right)\dot{\varepsilon}_{pl}$$

where $\dot{\varepsilon}_{pl}$ is the usual measure for the rate of accumulated plastic strain.

In material model 104 of LS-DYNA, the evolution rule of the damage variable D is given by:

$$\dot{D} = \begin{cases} 0 & for\ r \le r_D \\ \dfrac{\overline{y}}{S\left(1-D\right)}\dot{r} & for\ r > r_D \end{cases}$$

where r_D is the threshold for damage initiation, S is a positive material constant, and $\overline{y}$ is the release rate of strain energy density defined as:

$$\overline{y} = \frac{1}{2}\varepsilon^e : C : \varepsilon^e = \frac{\sigma_e^2 R_v}{2E\left(1-D\right)^2},$$

$$R_v = \frac{2}{3}\left(1+v\right) + 3\left(1-2v\right)\left(\frac{p}{\sigma_e}\right)^2$$

Here, R_v is referred to as the triaxiality function, v is the Poisson ratio, $p = -\frac{1}{3}\sigma_{kk}$ is the hydrostatic pressure, ε^e is the elastic strain tensor, C is the fourth order tensor of elastic moduli and σ_e is the von Mises stress. Finally, the rupture criterion of the facesheet material is given by $D = D_C$, where D_C is a material constant denoted as the critical damage.

The material data referring to the above equations are listed in Table 1.

Table 1: Material model 104 of LS_DYNA [13].

ρ	E	V	Y^0	Q_1	c_1
2700kg/m^3	70 GPa	0.3	364.5MPa	334.7MPa	6.16
r_D	S	D_C	Q_2	c_2	
0.18	0.5MPa	0.1	0MPa	0	

2.4 Constitutive description of cell wall material

The plastic properties of the cell wall material contribute significantly to the mechanical performance of the foam material. However, as the cell wall

microstructures are formed differently depending on the production processes and the composition of the cell wall material, measuring the precise values of cell wall material properties has long been a challenge.

Jeon *et al.* [14] proposed an approach to determine the mechanical properties of the cell wall material for closed-cell aluminium foams. Quasi-static uniaxial compression tests of the aluminum foam were firstly carried out. Subsequently, numerical simulations of the experimental process were then performed using the FE models. Finally, the mechanical properties of the cell wall material were determined by comparing the computed and measured force-displacement curves.

Using an approach similar to that of Jeon *et al.* [14], we obtained the isotropic hardening plasticity constitutive parameters of the cell wall material as: Young's modulus E = 70 GPa, Poisson ratio $v = 0.3$, yield stress $\sigma_Y = 132\,\text{MPa}$, tangent modulus 0, and failure strain 2.0 (to prevent excessive deformation of element), with the strain rate effects of the cell wall material ignored. Quasi-static compressive tests were performed on a displacement controlled servo-hydraulic test machine. The numerically predicted uniaxial compressive stress versus strain curve of the foam is presented in Fig. 3 together with that measured experimentally. It is seen from Fig. 3 that the fitting accuracy is acceptable, and that the homogeneous foam exhibits a near constant plateau stress typical for high porosity metallic foams. In contrast, if the FE model of Fig. 1 is adopted, the model predicts that the gradient-density foam exhibits a smoothly rising plateau stress as shown in Fig. 3.

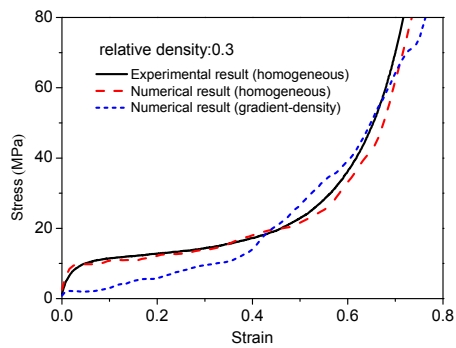

Figure 3: Numerically predicted and experimentally measured uniaxial compressive stress versus strain curves for closed-cell aluminum foams.

3 Results and discussion

Table 2 summarizes the present numerical predictions for both monolithic and sandwich beams. Here, $\bar{W} = W/L$ is the dimensionless maximum deflection, where W is the permanent deflection at the mid-span of the back facesheet;

$\varepsilon_c = \Delta c / c$ is the maximum average compressive strain of the foam core, where Δc is the maximum difference in mid-span deflections of the front and back facesheets.

Table 2: Summary of FE predictions for monolithic and sandwich beams.

Beam type (L=250mm)	Pressure (MPa)	Time (ms)	Impulse (kPa s)	$\bar{W}$	ε_c
Monolithic	100	0.03	3.0	0.071	--
Monolithic	100	0.06	6.0	0.127	--
Monolithic	100	0.09	9.0	0.188	--
homogeneous core	100	0.03	3.0	0.049	0.253
homogeneous core	100	0.06	6.0	0.121	0.568
homogeneous core	100	0.09	9.0	0.190	0.664
low-high gradient-density core	100	0.03	3.0	0.057	0.446
low-high gradient-density core	100	0.06	6.0	0.132	0.624
low-high gradient-density core	100	0.09	9.0	0.200	0.657
high-low gradient-density core	100	0.03	3.0	0.057	0.224
high-low gradient-density core	100	0.06	6.0	0.124	0.540
high-low gradient-density core	100	0.09	9.0	0.193	**3.661**

3.1 Deformation and failure modes for each type of beam

In calculations, the effects of applied impulse and core topology on the failure modes of sandwich beams were investigated. Note that, to focus on the details of core deformation, only the central portion of the beam is highlighted in Fig. 4. The dynamic response of the sandwich beams may be split into a sequence of three stages: upon applying the shock impulse, the front facesheet obtains an initial velocity while the rest of the beam is motionless (frame 1); subsequently, the foam core is compressed progressively on the upper side directly under shock loading while the back facesheet remains motionless (frames 2 and 3); the final stage is a retardation process wherein the beam is brought to rest by plastic bending and stretching, with plastic hinges travelling from the beam center (frame 4) towards the clamped edges (frame 7). Aluminum foams are known to have much lower fracture strength in tension/shear than that in compression.

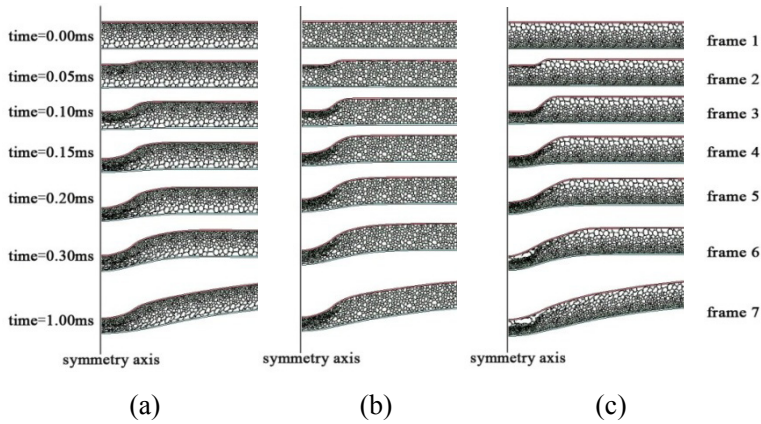

Figure 4: The selected deflection profiles of three sandwich beams (6.0kPa s) (a) high-low gradient-density core; (b)homogeneous core; (c) low-high gradient-density core

Consequently, during unloading, the foam core may fracture due to combined tensile and shear stressing. For the present sandwich beam with low-high gradient-density core, interfacial failure indeed occurs between the front facesheet and the low density foam core. Two deflected shapes of the sandwich beams are found to be bend dominated mode and stretch dominated mode according to the shock impulse level. The thin core often leads to the bend dominated mode of sandwich beams when the applied impulse is small (e.g. 3.0kPa s). When subjected to large impulse (e.g. 6.0kPa s), sandwich beams is found to be stretch dominated mode.

3.2 Maximum deflection for each type of beam

Despite the variation of deformation patterns mentioned above, the structural response of each type of beam may be represented by the maximum deflection of the mid-span. Furthermore, the maximum deformation is the major response of interest for its application as barriers for human or objects to shield from blast attacks.

For monolithic beams, the maximum deflection of the mid-point increases with applied impulse. When applied impulse keeps the same (e.g. 6.0kPa s), the various pressures versus corresponding time has negligible influence on the maximum deflection.

The sandwich beams outperform the solid monolithic beams at lower impulse levels (e.g. 3.0kPa s), wherein maximum deflections of the sandwich beam with homogeneous core are only about 69% of those for the solid beams, which is about a 31% decrease. At higher impulse levels (e.g. 6.0kPa s and 9.0 kPa s), the benefits diminish, the maximum deflections of the each beam are almost the same.

At studied impulse levels, sandwich beam with homogeneous core shows smallest mid-point deflection of back face sheet compared with sandwich beams with gradient-density aluminum foams cores. At lower impulse levels (3.0kPa s), sandwich beams with high-low or low-high gradient-density core show the same mid-point deflection, which is a little large than that with homogeneous core. At higher impulse levels (6.0kPa s and 9.0 kPa s), sandwich beam with low-high gradient-density core shows the largest mid-point deflection than two other type of beams. The best topology structure of cores in terms of the energy absorption capacity still is the homogeneous core.

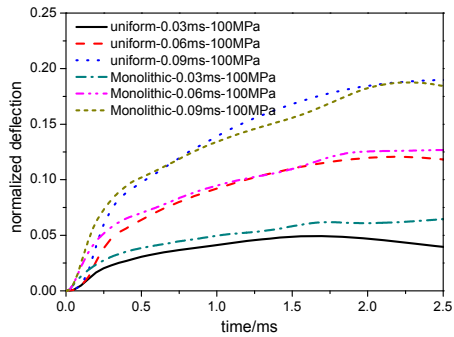

(a)

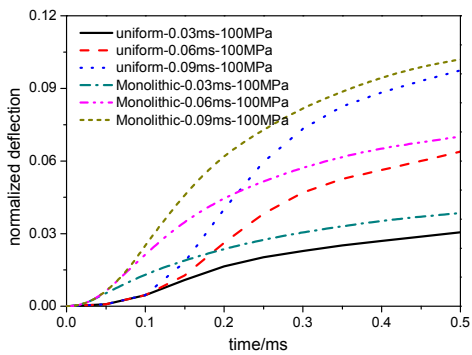

(b)

Figure 5: Maximum deflection-time history at the mid-span of monolithic and sandwich beams (a) entire view of 0.0–2.5ms; (b) enlarged view of 0.0–0.5ms.

The maximum deflection-time history at the mid-span of monolithic and sandwich beams is illustrated in Fig. 5. It is found that the beams spring back a small amount after it reached its maximum deflection. The deflection of sandwich beams at mid-span increases at a slower pace than that of monolithic beams.

3.3 Maximum average strain of cores for each type of beam

In addition, significant amounts of core crush were observed in the metal foam core sandwich beams loaded dynamically (see frame 2 in Fig. 4). The maximum average compressive strain of the core increases with applied impulse for three topology structures (Fig. 6). The beam with low-high gradient-density core shows the maximum average compressive strain, while smallest average compressive strain of aluminum foam cores occurs in sandwich beam with high-low gradient-density core. The core is compressed and the corresponding strain increases steeply and reaches the maximum value at approximately t=0.2ms.

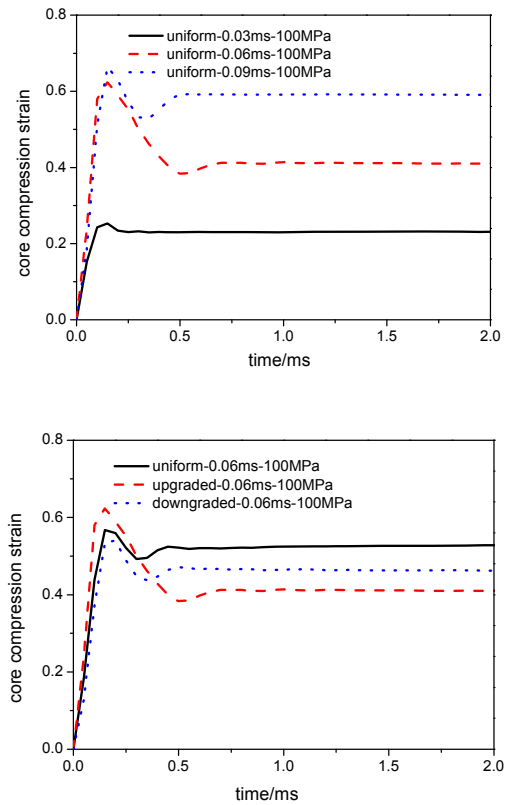

Figure 6: Maximum average strain-time history of cores for each type of beam.

4 Conclusions

Finite element simulations are presented for the dynamic shock responses of end-clamped sandwich beams consisted of aluminum facesheets and closed-cell

aluminum foam cores having gradient densities. Three types of core configurations, having identical areal density, are modeled as homogeneous core, low-high gradient density core and high-low gradient density core. The aluminum foams are analyzed using the mesoscopic FE models that represent the cell shape and geometric distribution of the real foam, with two-dimensional FE models created from tomographic images of the foam.

Depending upon the shock impulse level applied, the gradient foam-cored sandwich beam deforms in either bend or stretch dominated mode. Within the bend dominated domain, the sandwich beams outperform monolithic solid beams of equivalent mass. The benefits diminish as the deformation pattern of the sandwich beam becomes stretch dominated. For the three types of sandwich beam considered, that with homogeneous foam core exhibits the smallest mid-span deflection while that with low-high gradient core achieves the largest average compressive strain. As no experimental measured compressive stress-strain curves of gradient-density aluminum foams exist in the open literature, this and other relevant issues will be addressed in future studies.

References

[1] Radford, D.D., Deshpande, V.S. and Fleck, N.A., The use of metal foam projectiles to simulate shock loading on a structure. *International Journal of Impact Engineering*, **31(9)**, pp. 1152–1171, 2005.

[2] Radford, D.D., Fleck, N.A. and Deshpande, V.S., The response of clamped sandwich beams subjected to shock loading. *International Journal of Impact Engineering*, **32(6)**, pp. 968–987, 2006.

[3] Radford, D.D., McShane, G.J. and Deshpande, V.S., et al., The response of clamped sandwich plates with metallic foam cores to simulated blast loading. *International Journal of Solids and Structures*, **43(7–8)**, pp. 2243–2259, 2006.

[4] Daxner, T., Rammerstorfer, F.G. and Bohm, H.J., Adaptation of density distributions for optimising aluminium foam structures. *Materials Science and Technology*, **16(7–8)**, pp. 935–939, 2000.

[5] Brothers, A.H. and Dunand, D.C., Mechanical properties of a density-graded replicated aluminum foam. *Materials Science and Engineering A - Structural Materials Properties Microst,* **489(1–2)**, pp. 439–443, 2008.

[6] Wang, E.H., Gardner, N. and Shukla, A., The blast resistance of sandwich composites with stepwise graded cores. *International Journal of Solids and Structures*, **46(18–19)**, pp. 3492–3502, 2009.

[7] Zhao, H., Zeng, H.B. and Pattofatto, S., et al., Perforation of sandwich plates with graded hollow sphere cores under impact loading. *International Journal of Impact Engineering,* **37(11)**, pp. 1083–1091, 2010.

[8] Sun, G.Y., Li, G.Y. and Hou, S.J., et al., Crashworthiness design for functionally graded foam-filled thin walled structures. *Materials Science and Engineering A - Structural Materials Properties Microst*, **527(7–8)**, pp. 1911–1919, 2010.

[9] Silva, M.J., Hayes, W.C. and Gibson, L.J., The effects of nonperiodic microstructure on the elastic properties of 2-dimensional cellular solids. *International Journal of Mechanical Sciences*, **37**, pp. 1161–1177, 1995
[10] Kádár, C., Maire, E. and Borbély, A., et al., X-ray tomography and finite element simulation of the indentation behavior of metal foams. *Materials Science and Engineering A - Structural Materials Properties Microst,* **387**, pp. 321–325, 2004.
[11] Zhang, J., Zhao, G.P. and Lu, T.J., Experimental and numerical study on strain rate effects of close-celled aluminum foams, *Journal of Xi'an Jiaotong University*, **44(5)**, pp. 97–101, 2010.
[12] Hallquist, J.O., *LS-DYNA theoretical manual*. Livermore Software Technology Corporation, 2005.
[13] Hanssen, A.G., Girard, Y. and Olovsson, L., et al., A numerical model for bird strike of aluminum foam-based sandwich panels. International Journal of Impact Engineering, **32(7)**, pp. 1127–1144, 2006.
[14] Jeon, I., Katou, K. and Sonoda, T., et al., Cell wall mechanical properties of closed-cell Al foam. *Mechanics of Materials*, **41**, pp. 60–73, 2009.